Article

Mechanism of Water Photooxidation Reaction at Atomically Flat TiO (Rutile) (110) and (100) Surfaces: Dependence on Solution pH

Akihito Imanishi, Tomoaki Okamura, Naomichi Ohashi, Ryuhei Nakamura, and Yoshihiro Nakato

J. Am. Chem. Soc., **2007**, 129 (37), 11569-11578• DOI: 10.1021/ja073206+ • Publication Date (Web): 28 August 2007

J|A|C|S
ARTICLES
Published on Web 08/28/2007

Mechanism of Water Photooxidation Reaction at Atomically Flat TiO_2 (Rutile) (110) and (100) Surfaces: Dependence on Solution pH

Akihito Imanishi,*[,†,‡] Tomoaki Okamura,[†] Naomichi Ohashi,[†] Ryuhei Nakamura,[§] and Yoshihiro Nakato[‡,||]

Contribution from the Division of Chemistry, Graduate School of Engineering Science, Osaka University, Toyonaka, Osaka 560-8531, Japan, Department of Applied Chemistry, School of Engineering, The University of Tokyo, Hongo, Bunkyo-ku, Tokyo 113-8656, Japan, The Institute of Scientific and Industrial Research (ISIR), Osaka University, Ibaraki, Osaka, 567-0047 Japan, and Core Research for Evolutional Science and Technology (CREST), JST, Tokyo, Japan

Received May 17, 2007; E-mail: imanishi@chem.es.osaka-u.ac.jp

Abstract: The mechanism of water photooxidation reaction at atomically flat n-TiO_2 (rutile) surfaces was investigated in aqueous solutions of various pH values, using photoluminescence (PL) measurements. The PL bands, which peaked at around 810 and 840 nm for the (110) and (100) surfaces, respectively, were assigned to radiative transitions between conduction-band electrons and surface-trapped holes (STH), $[Ti-O=Ti_2]_s^+$, formed at triply coordinated (normal) O atoms at the surface lattice. The PL intensity (I_{PL}) decreased stepwise with increasing solution pH, namely, it sharply decreased at around pH 4, near the point of zero charge of TiO_2 (about 5), and then rapidly decreased to zero near pH 13. The first sharp decrease around pH 4 is attributed to the increased rate of nucleophilic attack of a water molecule to a hole at a site of surface bridging oxygen (Ti−O−Ti), the density of which increases with increasing pH. The nucleophilic attack is regarded as the main initiating step of the water oxidation reaction in low and intermediate pH. The high PL intensity at low pH is ascribed to slow nucleophilic attack owing to a very low density of Ti−O−Ti by its protonation at the low pH. The second sharp decrease near pH 13 is attributed to formation of surface anionic species like $Ti-O^-$ which can be readily oxidized by photogenerated holes. Interrelations between reaction intermediates proposed in this work and those reported by time-resolved laser spectroscopy are discussed.

Introduction

The oxygen photoevolution (or water photooxidation) reaction on TiO_2 and related metal oxides[1−8] or oxynitrides[9,10] has been attracting strong attention from the point of view of solar water splitting. This reaction has also attracted much attention in view of photocatalytic environmental cleaning[11−15] because intermediate radicals of this reaction play a crucial role in photodecomposition of soiling or harmful organic compounds. In particular, keen attention has recently been paid to development of visible-light responsive metal oxides or oxynitrides with an aim at efficient solar decomposition of water[3−10] and organic compounds.[16−26] For exploring new visible-light active materi-

† Graduate School of Engineering Science, Osaka University.
‡ CREST, JST.
§ School of Engineering, The University of Tokyo.
|| ISIR, Osaka University.

(1) Fujishima, A.; Honda, K. *Nature* **1972**, *238*, 37−38.
(2) Domen, K.; Naito, S.; Soma, M.; Onishi, T.; Tamaru, K. *Chem. Commun.* **1980**, 543.
(3) Sato, S.; White, J. M. *Chem. Phys. Lett.* **1980**, *72*, 83−86.
(4) Zou, Z. G.; Ye, J.; Sayama, K.; Arakawa, H. *Nature* **2001**, *414*, 625.
(5) Kato, H.; Asakura, K.; Kudo, A. *J. Am. Chem. Soc.* **2003**, *125*, 3082−3089.
(6) Kudo, A.; Kato, H.; Tsuji, I. *Chem. Lett.* **2004**, *33*, 1354−1355.
(7) Liu, H. M.; Nakamura, R.; Nakato, Y. *Chem. Phys. Chem.* **2005**, *6*, 2499−2502.
(8) Liu, H. M.; Nakamura, R.; Nakato, Y. *Electrochem. Solid-State Lett.* **2006**, *9*, G187−G190.
(9) Hara, M.; Hitoki, G.; Takata, T.; Kondo, J. N.; Kobayashi, H.; Domen, K. *Catal. Today* **2003**, *78*, 555−560.
(10) Maeda, K.; Teramura, K.; Lu, D.; Takata, T.; Saito, N.; Inoue, Y.; Domen, K. *Nature* **2006**, *440*, 295.
(11) Ollis, D. S.; Al-Ekabi, H. *Photocatalytic Purification and Treatment of Water and Air*; Elsevier: Amsterdam, 1992.
(12) Fujishima, A.; Rao, T. N.; Tryk, D. A. *J. Photochem. Photobiol., C: Photochem. Rev.* **2000**, *1*, 1−21.
(13) Hoffmann, M. R.; Martin, S. T.; Choi, W. Y.; Bahnemann, D. W. *Chem. Rev.* **1995**, *95*, 69−96.
(14) Linsebigler, A. L.; Lu, G.; Yates, J. T., Jr. *Chem. Rev.* **1995**, *95*, 735−758.
(15) Wang, R.; Hashimoto, K.; Chikuni, M.; Kojima, E.; Kitamura, A.; Shimohigashi, M.; Watanabe, T. *Nature* **1997**, *388*, 431−432.
(16) Asahi, R.; Morikawa, T.; Ohwaki, T.; Aoki, K.; Taga, Y. *Science* **2001**, *293*, 269−271.
(17) Barborini, E.; Conti, A. M.; Kholmanov, I.; Piseri, P.; Podesta, A.; Milani, P.; Cepek, C.; Sakho, O.; Macovez, R.; Sancrotti, M. *Adv. Mater.* **2005**, *17*, 1842−1846.
(18) Burda, C.; Lou, Y.; Chen, X.; Samia, A. C. S.; Stout, J.; Gole, J. L. *Nano Lett.* **2003**, *3*, 1049−1051.
(19) Sakthivel, S.; Janczarek, M.; Kisch, H. *J. Phys. Chem. B* **2004**, *108*, 19384−19387.
(20) Ohno, T.; Mitsui, T.; Matsumura, M. *Chem. Lett.* **2003**, *32*, 364−365.
(21) Zhao, W.; Ma, W.; Chen, C.; Zhao, J.; Shuai, Z. *J. Am. Chem. Soc.* **2004**, *126*, 4782−4783.
(22) Irie, H.; Watanabe, Y.; Hashimoto, K. *J. Phys. Chem. B* **2003**, *107*, 5483−5486.
(23) Diwald, O.; Thompshon, T. L.; Zubkov, T.; Goralski, E. G.; Walck, S. D.; Yates, J. T., Jr. *J. Phys. Chem. B* **2004**, *108*, 6004−6008.

als, it is of key importance to elucidate molecular mechanisms of the reactions, which should strongly depend on the morphological, chemical, and electronic structures of materials at the surface as well as the reactivity (or energy) of photogenerated holes.[27−29] Such studies will also serve for research to lower high overvoltages in the oxygen evolution at metallic electrodes.

It has long been assumed[11−13,30−44] that the water photooxidation reaction at the TiO_2 surface is initiated by oxidation of surface Ti−OH group (or OH^- ions in an aqueous solution) by photogenerated holes, h^+, by an electron-transfer mechanism.[45,46]

$$Ti{-}OH_s + h^+ \rightarrow [Ti \cdot OH]_s^+ \quad (1)$$

The formation of ·OH radicals in UV-irradiated TiO_2 systems was reported by a spin-trapping ESR[30,40] or low-temperature ESR[36] method, diffuse reflection FTIR spectroscopy,[42] and gas-phase emission spectroscopy.[47] However, it was reported[48] that the water photooxidation reaction at the TiO_2 surface did not produce any free ·OH radicals but adsorbed ·OH (or Ti−O•) radicals, the latter of which gave ESR signals similar to those reported by the spin-trapping method. It was also reported[49] that ·OH radicals were produced from hydrogen peroxide (H_2O_2) formed via reduction of molecular oxygen by electrons in the conduction band. Moreover, recent theoretical calculation has shown[50] that surface Ti(OH) groups can act as electron traps but cannot act as hole traps by formation of $Ti^{4+}(OH)^•$ radicals, O 2p orbitals of surface Ti(OH) being entirely mixed with the O 2p orbitals of the valence band.

On the other hand, we have recently reported[51−54] that the water photooxidation reaction is not initiated by the electron-transfer oxidation of Ti−OH but by a nucleophilic attack of an H_2O molecule (Lewis base) to a surface-trapped hole (STH, Lewis acid). The processes are schematically expressed, including the results of this work, as follows:

$$[Ti_2{=}O{-}Ti]_s + h^+ \rightarrow [Ti_2{=}O\cdots Ti]^+_s$$
surface-trapped hole, STH (2)

$$[Ti_2{=}O\cdots Ti]^+_s \text{ ····· } \rightarrow \text{diffusion along terrace} \quad (3)$$

$$[Ti_2{=}O\cdots Ti]^+_s + [Ti{-}O{-}Ti]_s + H_2O \rightarrow [Ti_2{=}O{-}Ti]_s + [Ti{-}O^• HO{-}Ti]_s + H^+ \quad (4)$$

Here $[Ti_2{=}O{-}Ti]_s$ and $[Ti{-}O{-}Ti]_s$ refer to a triply coordinated (normal) O atom and a bridging O atom at the surface, respectively (see species a and c of Figure 10). Reaction 4 implies that an H_2O molecule attacks to a site of bridging O atom, $[Ti{-}O{-}Ti]_s$, accompanied by transfer of a hole from $[Ti_2{=}O\cdots Ti]^+_s$ in a concerted manner. The STH can be regarded as a relaxed hole at the surface, formed by orientational polarization of water molecules in solution as well as crystal lattice relaxation against bond lengthening caused by trapping a hole (one-electron deficiency). Though reaction 4 might be the main process, it cannot be excluded completely that a photogenerated hole before relaxation directly reacts with water at bridging oxygen:

$$h^+ + [Ti{-}O{-}Ti]_s + H_2O \rightarrow [Ti{-}O^• HO{-}Ti]_s + H^+ \quad (5)$$

Further details of the mechanism for the water photooxidation reaction are shown in Scheme 1.

In relation with the above mechanism, we also reported[55−61] that the n-TiO_2 rutile electrode showed a PL band peaked at around 840 nm, which was assigned to an electronic transition via an intermediate of the water photooxidation reaction. This assignment was given support by experiments on PL quenching by reductants added to the electrolyte, in which a reductant which quenched the PL efficiently suppressed the oxygen photoevolution effectively as well.[60] Our later work[53,54] has shown that the atomically flat TiO_2 rutile (110) and (100) surfaces emit the PL bands peaked at about 810 and 840 nm, respectively, both of which can be assigned to radiative

(24) Kahn, S. U. M.; Al-Shahry, M.; Ingler, W. B., Jr. *Science* **2002**, *297*, 2243−2245.
(25) Sakthivel, S.; Kisch, H. *Angew. Chem., Int. Ed.* **2003**, *42*, 4908−4911.
(26) Neumann, B.; Bogdanoff, P.; Tributsch, H.; Sakthivel, S.; Kisch, H. *J. Phys. Chem. B* **2005**, *109*, 16579−16586.
(27) Nakamura, R.; Tanaka, T.; Nakato, Y. *J. Phys. Chem. B* **2004**, *108*, 10617−10620.
(28) Nakamura, R.; Tanaka, T.; Nakato, Y. *J. Phys. Chem. B* **2005**, *109*, 8920−8927.
(29) Liu, H. M.; Imanishi, A.; Nakato, Y. *J. Phys. Chem. C* **2007**, *111*, 8603−8610.
(30) Jaeger, C. D.; Bard, A. J. *J. Phys. Chem.* **1979**, *83*, 3146−3152.
(31) Sato, S.; White, J. M. *J. Am. Chem. Soc.* **1980**, *102*, 7206−7210.
(32) Salvador, P.; Gutiérrez, C. *Chem. Phys. Lett.* **1982**, *86*, 131−134.
(33) Salvador, P.; Gutiérrez, C. *Surf. Sci.* **1983**, *124*, 398−406.
(34) Salvador, P.; Gutiérrez, C. *J. Phys. Chem.* **1984**, *88*, 3696−3698.
(35) Salvador, P.; Gutiérrez, C. *J. Electroanal. Chem.* **1984**, *160*, 117−130.
(36) Anpo, M.; Shima, T.; Kubokawa, Y. *Chem. Lett.* **1985**, 1799−1802.
(37) Norton, A. P.; Bernasek, S. L.; Bocarsly, A. B. *J. Phys. Chem.* **1988**, *92*, 6009−6016.
(38) Lawless, D.; Serpone, N.; Meisel, D. *J. Phys. Chem.* **1991**, *95*, 5166−5170.
(39) Gerischer, H. *Electrochim. Acta* **1993**, *38*, 3−9.
(40) Schwarz, P. F.; Turro, N. J.; Bossmann, S. H.; Braun, A. M.; Wahab, A.-M. A. A.; Dürr, H. *J. Phys. Chem. B* **1997**, *101*, 7127−7134.
(41) Kesselman, J. M.; Weres, O.; Lewis, N.; Hoffmann, M. R. *J. Phys. Chem. B* **1997**, *101*, 2637−2643.
(42) Szczepankiewicz, S. H.; Colussi, J. A.; Hoffmann, M. R. *J. Phys. Chem. B* **2000**, *104*, 9842−9850.
(43) Park, J. S.; Choi, W. *Langmuir* **2004**, *20*, 11523−11527.
(44) Ferguson, M. A.; Hoffmann, M. R.; Hering, J. G. *Environ. Sci. Technol.* **2005**, *39*, 1880−1886.
(45) Gerischer, H. In *Physical Chemistry, An Advanced Treatise*; Eyring, H., Ed.; Academic Press: New York, 1970; Vol. 9A, p 463.
(46) Nozik, A. J.; Memming, R. *J. Phys. Chem.* **1996**, *100*, 13061−13078.
(47) Murakami, Y.; Kenji, E.; Nosaka, A. Y.; Nosaka, Y. *J. Phys. Chem. B.* **2006**, *110*, 16808−16811.
(48) Nosaka, Y.; Komori, S.; Yawata, K.; Hirakawa, T.; Nosaka, Y. A. *Phys. Chem. Chem. Phys.* **2003**, *5*, 4731−4735.
(49) Kubo, W.; Tatsuma, T. *J. Am. Chem. Soc.* **2006**, *128*, 16034−16035.
(50) Valentin, C. D.; Pacchioni, G. *Phys. Rev. Lett.* **2006**, *97*, 166803(1)−(4).
(51) Kisumi, T.; Tsujiko, A.; Murakoshi, K.; Nakato, Y. *J. Electroanal. Chem.* **2003**, *545*, 99−107.
(52) Nakamura, R.; Nakato, Y. *J. Am. Chem. Soc.* **2004**, *126*, 1290−1298.
(53) Nakamura, R.; Ohashi, H.; Imanishi, A.; Osawa, T.; Matsumoto, Y.; Koinuma, H.; Nakato, Y. *J. Phys. Chem. B* **2005**, *109*, 1648−1651.
(54) Nakamura, R.; Okamura, T.; Ohashi, N.; Imanishi, A.; Nakato, Y. *J. Am. Chem. Soc.* **2005**, *127*, 12975−12983.
(55) Nakato, Y.; Tsumura, A.; Tsubomura, H. *Chem. Phys. Lett.* **1982**, *85*, 387−390.
(56) Nakato, Y.; Tsumura, A.; Tsubomura, H. *J. Phys. Chem.* **1983**, *87*, 2402−2405.
(57) Nakato, Y.; Ogawa, H.; Morita, K.; Tsubomura, H. *J. Phys. Chem.* **1986**, *86*, 6210−6216.
(58) Nakato, Y.; Akanuma, H.; Shimizu, J.-I.; Magari, Y. *J. Electroanal. Chem.* **1995**, *396*, 35−39.
(59) Magari, Y.; Ochi, H.; Yae, S.; Nakato, Y. *Solid/Liquid Electrochemical Interfaces;* ACS Symposium Series No. 656; The American Chemical Society: Washington, DC, 1997; pp 297−309.
(60) Nakato, Y.; Akanuma, H.; Magari, Y.; Yae, S.; Shimizu, J.-I.; Mori, H. *J. Phys. Chem. B* **1997**, *101*, 4934−4939.
(61) Tsujiko, A.; Kisumi, T.; Magari, Y.; Murakoshi, K.; Nakato, Y. *J. Phys. Chem. B* **2000**, *104*, 4873−4879.

Scheme 1

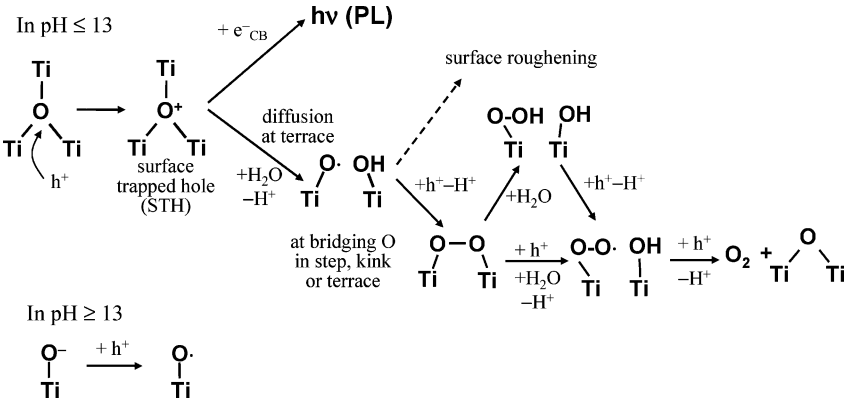

recombination transitions between conduction-band electrons (e^-_{CB}) and the surface-trapped holes (STH):

$$[Ti_2{=}O\cdots Ti]^+_s + e^-_{CB} \rightarrow PL \qquad (6)$$

Interestingly, the PL bands were observed only for the atomically flat surfaces and never observed for atomically nonflat surfaces, e.g., commercially available (110)- or (100)-cut surfaces.[53,54] Processes (4)−(6) indicate that the water photooxidation reaction and photoluminescent process are competitive with each other, implying that the mechanism of the water photooxidation reaction can be investigated by PL measurements.

The new mechanism for the water photooxidation reaction, expressed by reactions 2−6, was verified by a number of experimental results.[51−54] In particular, in situ multiple internal reflection FTIR spectroscopy[52] together with ^{18}O isotope exchange experiments clearly showed that lattice oxygen was incorporated in a surface reaction intermediate of peroxide type, Ti−O−O−Ti, which was only explained by assuming reaction 4 or 5. In addition, experiments with atomically flat (110) and (100) n-TiO_2 (rutile) surfaces in low and intermediate pH regions[54] showed that atomic level surface roughening occurred with the progress of oxygen photoevolution reaction, which could never be explained by reaction 1 or related processes in which no breaking of Ti−O bonds was induced at the surface lattice. The new mechanism was also supported by many reported results: Howe and Grätzel[62] reported by ESR measurements that photogenerated holes were trapped at lattice O atoms at low temperatures of 4.2 or 77 K, not producing ·OH radicals. Micic et al.[63,64] also clearly showed that UV illumination of TiO_2 did not produce ·OH radicals but Ti−O· radicals, in harmony with the mechanism of reaction 4 or 5. Hashimoto et al.[65] also reported, by measuring the quantum yield of formation of ·OH radicals by means of a fluorescence probe method, that the formation of ·OH radicals was not be the major process on irradiated TiO_2 (anatase) in aqueous solutions.

The estimation of energy levels of occupied O 2p orbitals for surface oxygen species is an important issue for investigating the mechanism. In a previous paper,[52] the top of the O 2p level for surface Ti−OH−Ti and Ti−OH under vacuum was estimated, using reported UPS spectra,[66−68] to be about 3.7 and 1.8 eV below the top of the valence band at the surface, E_v^s, respectively, as shown in Figure 1. The top of the O 2p level for Ti−OH−Ti and Ti−OH at the TiO_2/water interface, after consideration of stabilization by electronic polarization of solvent water, was still about 2.6 and 0.7 eV below the E_v^s [52] (Figure 1). These estimations are supported by the fact that XPS O 1s peaks for surface Ti−OH and Ti−O−Ti of TiO_2 are at about 2.6 and 1.2 eV higher energies than the peak for lattice O atoms.[69−71] The O 2p levels for solution species, H_2O_{aq} and OH^-_{aq}, can be estimated by using photoelectron emission spectra of aqueous solutions reported by Delahay et al.,[72] together with estimated standard redox potentials, $E^0(OH^-_{aq}/OH^\bullet_{aq}) = 1.55$ V vs NHE,[73] $E^0(H_2O_{aq}/OH^\bullet_{aq} + H^+_{aq}) = 2.38$ V,[73,74] and $E^0(H_2O_{aq}/H_2O^+_{aq}) = 3.3$ V.[72] Though the $E^0(OH^-_{aq}/OH^\bullet_{aq})$ and $E^0(H_2O_{aq}/OH^\bullet_{aq} + H^+_{aq})$ are above the E_v^s at pH 0 (Figure 1), the reorganization energies for the electron transfer are so large that the effective O 2p levels for OH^-_{aq} and H_2O_{aq}, $D_R(E^0, \lambda)$, determined by the photoelectron emission spectra, are far below the E_v^s at pH 0 (Figure 1). Note also that the concentration of OH^-_{aq} is negligibly small in pH ≤ 9 and that the increase in pH shifts the E_v^s upward at a rate of −0.059 V/pH. Thus, all the surface O species have the O 2p levels below the E_v^s and cannot be oxidized by the valence-band holes by the electron-transfer mechanism, indicating the nonvalidity of the conventional mechanism (reaction 1). Micic et al. reported[63] the following reaction instead of reaction 1:

$$Ti{-}OH_s + h^+ \rightarrow [Ti\ {\cdot}O]_s + H^+_{aq} \qquad (1')$$

Indeed, reaction 1′ is more plausible than reaction 1 because it is assisted by large hydration energy for H^+_{aq}. However, reaction 1′ can also not explain the aforementioned results of the incorporation of lattice oxygen into a reaction intermediate[52]

(62) How, R. F.; Gräetzel, M. *J. Phys. Chem.* **1987**, *91*, 3906−3909.
(63) Micic, O. I.; Zhang, Y.; Cromack, K. R.; Trifunac, A. D.; Thurnauer, M. C. *J. Phys. Chem.* **1993**, *97*, 7277−7283.
(64) Micic, O. I.; Zhang, Y.; Cromack, K. R.; Trifunac, A. D.; Thurnauer, M. C. *J. Phys. Chem.* **1993**, *97*, 13284−13288.
(65) Ishibashi, K.; Fujishima, A.; Watanabe, T.; Hashimoto, K. *J. Photochem. Photobiol., A* **2000**, *134*, 139−142.
(66) Brookes, I. M.; Muryn, C. A.; Thornton, G. *Phys. Rev. Lett.* **2001**, *87*, 266103(1)−(4).
(67) Muryn, C. A.; Hardman, P. J.; Crouch, J. J.; Raiker, G. N.; Thornton, G. D.S.L. law, *Surf. Sci.* **1991**, *251−252*, 747−752.
(68) Henderson, M. A. *Surf. Sci. Rep.* **2002**, *46*, 1−308.
(69) Xu, B.; Jing, L.; Ren, Z.; Wang, B.; Fu, H. *J. Phys. Chem. B* **2005**, *109*, 2805−2809.
(70) Yu. J. C.; Yu, J.; Zhao, J. J. *Appl. Catal., B* **2002**, *36*, 31−43.
(71) Sham, T. K.; Lazarus, M. S. *Chem. Phys. Lett.* **1979**, *68*, 426−432.
(72) Delahay, P.; Von Burg, K. *Chem. Phys. Lett.* **1981**, *83*, 250−254.
(73) Bard, A. J. *Standard potentials in aqueous solution*; Marcel Dekker Inc.: New York, 1985.
(74) *Electrochemical Handbook*, 5th ed.; The Electrochemical Society of Japan, Maruzen: Tokyo, 2000.

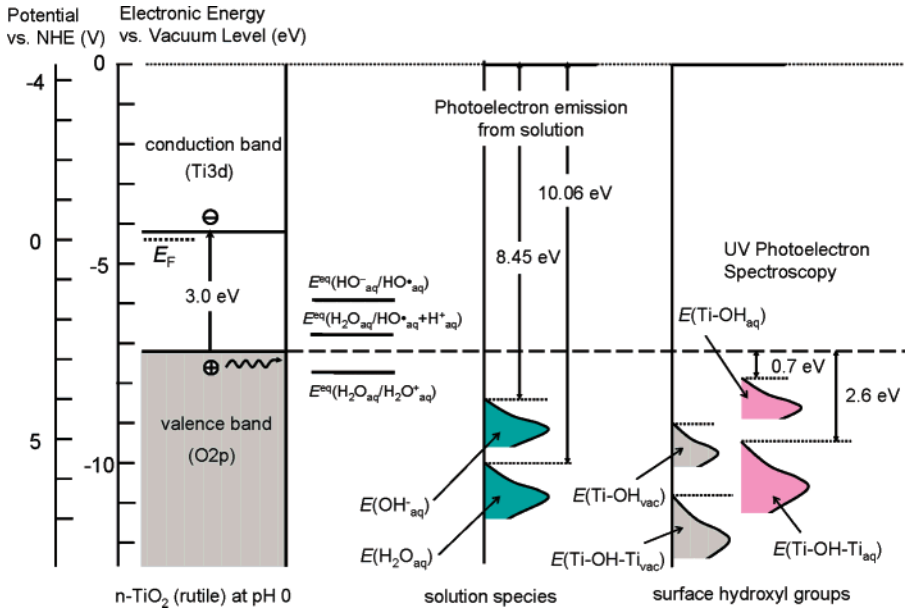

Figure 1. Energy levels of O 2p orbitals for oxygen species at the TiO_2 surface estimated from UPS and photoelectron emission spectra, compared with the conduction and valence bands of n-TiO_2 at pH 0. See text for details.

as well as photoinduced surface roughening.[54] Further details will be discussed again in the Discussion.

The new mechanism has important implications for exploring new visible-light responsive materials for oxygen evolution, because it belongs to Lewis acid−base reactions and has energetics and kinetics quite different from those for the electron-transfer reaction such as reaction 1. Namely, the new mechanism opens a new possibility for the development of visible-light induced water oxidation. Thus, the further confirmation of the mechanism is very important. In this work, we have investigated the effect of solution pH on the mechanism of the water photooxidation reaction, because the reaction rate is expected to depend strongly on solution pH owing to the occurrence of protonation or deprotonation in surface oxygen species with pH change.[75] Our previous work was mainly restricted to acidic solutions,[51,53,54] except in situ FTIR studies in neutral solutions.[52]

Experimental Section

Single-crystal TiO_2 (rutile) wafers of 10 mm × 10 mm in area and 1.0 mm thick, having the (100)- and (110)-cut and alkali-polished surfaces, were obtained from Earth Chemical Co., Ltd. The wafers were doped with 0.05 wt % niobium oxide and of n-type as they were, with no pretreatment, because doped Nb^{4+} acted as an electron donor. The atomically flat surfaces were obtained by a procedure of washing with acetone, immersing in 20% HF for 10 min, washing with water, and annealing at a temperature from 550 to 600 °C for 1−2 h in air.[53,54] X-ray photoelectron spectroscopic (XPS) analysis showed that no fluorine atom remained at the surface after the above procedure. Electrodes of n-TiO_2 were prepared by obtaining an Ohmic contact with indium−gallium alloy.

Photocurrent density (j) vs potential (U) curves for the n-TiO_2 electrodes were measured with a commercial potentiostat and a potential programmer, using a Pt plate as the counter electrode and an Ag/AgCl/KCl_{sat} electrode as the reference electrode. The photoluminescence (PL) intensity (I_{PL}) vs U was measured using a photomultiplier (Hamamatsu, R316 or R712) cooled at −20 °C together with a monochromator (Jobin Yvon, H20IR) or cutoff filters, whereas PL spectra were obtained with a multichannel photodiode array detector (Hamamatsu, PMA100) cooled at −20 °C. The I_{PL} vs U was measured simultaneously with the measurement of the j vs U. In both cases, the illumination was carried out by use of a 365 nm band from a 500 W high-pressure mercury lamp, obtained with band-pass filters. The intensity of the UV light was adjusted by a combination of neutral density (metal net) filters and measured with a thermopile (Eppley Laboratory). In this work, the low-intensity UV irradiation (0.2 mW/cm^2) was in most cases adopted because our previous experiments[54] have revealed that morphological roughening on an atomic level at the surface occurs even in 0.1 M $HClO_4$ especially under high-intensity (>1.0 mW/cm^2) and long-term (>0.5 C/cm^2) illumination. The surface roughening was suppressed to a negligible extent under low-intensity short-period irradiation.

Electrolyte solutions were prepared by use of reagent grade chemicals and pure water, the latter of which was obtained from deionized water with a Milli-Q water purification system. The solution pH was adjusted by using 0.1 M $HClO_4$, 1.0 M NaOH, and their mixtures. No agent for pH buffer was used to avoid influences of specific adsorption of multivalent anions. For minimizing a pH change near the electrode surface, the j vs U and I_{PL} vs U were measured by the first potential sweep from negative to positive, with the solution being stirred magnetically. Before the measurements, the electrolyte solution was bubbled with N_2 gas to remove dissolved O_2.

The morphology of the TiO_2 surfaces was inspected with an atomic force microscope (AFM, Digital Instruments NanoScope IIIa) at room temperature, the sample being placed in air. All AFM images were obtained in a tapping mode with a silicon tip (Digital Instruments) at a driving frequency of about 280 kHz and a scan rate of 1.5 Hz. The surface crystallinity was investigated by a low-energy electron diffraction (LEED) method.

Results

AFM inspection showed that the n-TiO_2 (rutile) (110) and (100) surfaces after the surface-flattening pretreatment (i.e., the immersion in 20% HF for 10 min, followed by annealing at 600 °C for 1 h) had clear step and terrace structures[53,54] (see also Figure 7), indicating that atomically flat (100) and (110) surfaces were obtained. The observed step height was 0.27 nm

(75) Connor, P. A.; Dobson, K. D.; McQuillan, A. J. *Langmuir* **1999**, *15*, 2402−2408.

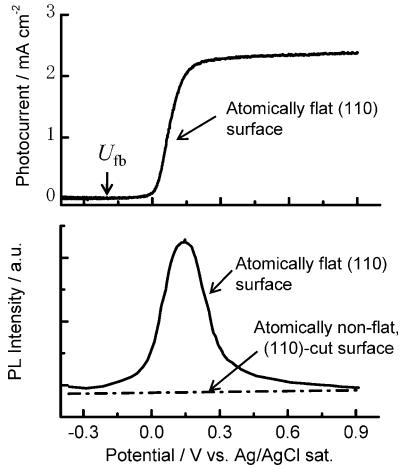

Figure 2. j vs U for an n-TiO_2 rutile electrode with the atomically flat (110) surface in 0.1 M $HClO_4$ (pH 1.1), compared with the PL intensity (I_{PL}) vs U. The I_{PL} vs U for an atomically nonflat surface is also included for reference. U_{fb}: flat-band potential.

for the (100) surface and 0.35 nm for the (110) surface, both in good agreement with the values in crystal lattice model of TiO_2 (rutile). The terrace width was about 200−300 nm in both the surfaces. The atomic level flatness of both the (110) and (100) surfaces was also shown by LEED measurements, which gave sharp intense (1 × 1) LEED spots.[53] Moreover, the formation of well-defined TiO_2 (100) and (110) surfaces was demonstrated by the fact that the flat-band potential (U_{fb}), determined by Mott−Schottky plots, as well as the onset potential of the photocurrent (U_{on}) showed clear differences of about 0.09 V between the (110) and (100) surfaces,[53,54] in agreement with the difference in the work function between them.[76] It is to be noted also that the flat (110) and (100) surfaces in this work were stable even under exposition to aqueous solutions of pH 1−14,[53,54] contrary to atomically flat TiO_2 surfaces prepared by the Ar^+-ion sputtering and thermal annealing under UHV conditions.[77]

Figure 2 shows, for later discussion, the reported j vs U and I_{PL} vs U for an n-TiO_2 rutile electrode with the atomically flat (110) surface in 0.1 M $HClO_4$ (pH 1.1).[53,54] The flat-band potential (U_{fb}) for the n-TiO_2(110) surface (−0.25 ± 0.01 V vs Ag/AgCl/sat. KCl at pH 1.1)[53,54] is also indicated for reference. A large positive deviation of the onset potential of the photocurrent, U_{on}, from the U_{fb} is attributed to efficient surface carrier recombination via surface states. The I_{PL} took a maximum near the U_{on} (Figure 2), indicating that the PL is really arising from surface carrier recombination (i.e., radiative recombination between conduction-band electrons, e^-_{CB}, and the surface-trapped holes, STH), as mentioned in the Introduction. The disappearance of the PL at positive potentials is simply attributed to increased band bending in the n-TiO_2 electrode, whereas that at negative potentials can be attributed to formation of reduced surface species, such as Ti^{3+},[53,54,60] which can trap efficiently the valence-band holes nonradiatively. Results similar to those of Figure 2 were obtained for an atomically flat TiO_2 (100) surface, with slight negative shifts in the j vs U and I_{PL} vs U. However, no PL was observed for atomically nonflat TiO_2 surfaces (Figure 2).[53,54]

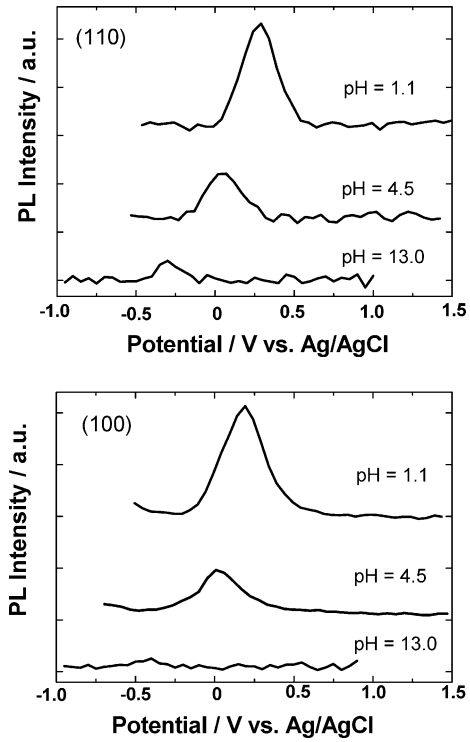

Figure 3. I_{PL} vs U for the n-TiO_2 (110) and (100) surfaces in solutions of various pH. The UV irradiation intensity was 0.2 mW/cm^2.

Figure 3 shows the I_{PL} vs U for the n-TiO_2 electrodes with the atomically flat (a) (110) and (b) (100) surfaces in solutions of various pH. The low-intensity UV irradiation of 0.2 mW/cm^2 was adopted to avoid the aforementioned surface roughening during the PL measurements. In all the solutions, the I_{PL} took the maximum near the U_{on}, in a manner similar to the case of Figure 2. The potential region where the PL was observed, as well as the U_{on}, shifted toward the negative with increasing the pH of the electrolyte, owing to the well-known shift of the U_{fb} at a rate of −0.059 V/pH at 300 K. A prominent feature of Figure 3 is that the I_{PL} drastically decreased with increasing the pH for both the (110) and (100) surfaces.

The detailed pH dependences of the I_{PL} at the peaked potential for the (110) and (100) TiO_2 surfaces, obtained under the low-intensity UV irradiation of 0.2 mW/cm^2, are shown in Figure 4, where the I_{PL} at pH 1.1 is normalized to unity in both the surfaces. The I_{PL} was the highest in an acidic solution (pH 1.1) and decreased stepwise with increasing the pH; namely, the I_{PL} sharply decreased at around pH 4 and at about pH 13. It is to be noted that pH 4.0 is close to the point of zero charge (pzc) of rutile TiO_2 (about 5.0) reported.[75,78,79]

Figure 5 compares the PL spectra in 0.1 M $HClO_4$ (pH 1.1) and 0.1 M NaOH (pH 13.0) for both the (110) and (100) surfaces, obtained under the UV irradiation intensity of 1.0 mW/cm^2 at potentials at which the I_{PL} took a maximum. The I_{PL} at the maximum wavelength is normalized to the same level between pH 1.1 and 13.0 to make clear the difference in the spectral position and shape. The PL bands from the (110) and (100) surfaces (not corrected for the spectral sensitivity of the multichannel photodiode detector) are peaked at about 810 and 840 nm, respectively, indicating that the energy level of the

(76) Imanishi, A.; Tsuji, E.; Nakato, Y. *J. Phys. Chem. C* **2007**, *111*, 2128−2132.
(77) Uetsuka, H.; Sasahara, A.; Onishi, H. *Langmuir* **2004**, *20*, 4782−4783.
(78) Bullard, J. W.; Cima, M. J. *Langmuir* **2006**, *22*, 10264−10271.
(79) Dobson, K. D.; Connor, P. A.; McQuillan, A. J. *Langmuir* **1997**, *13*, 2614−2616.

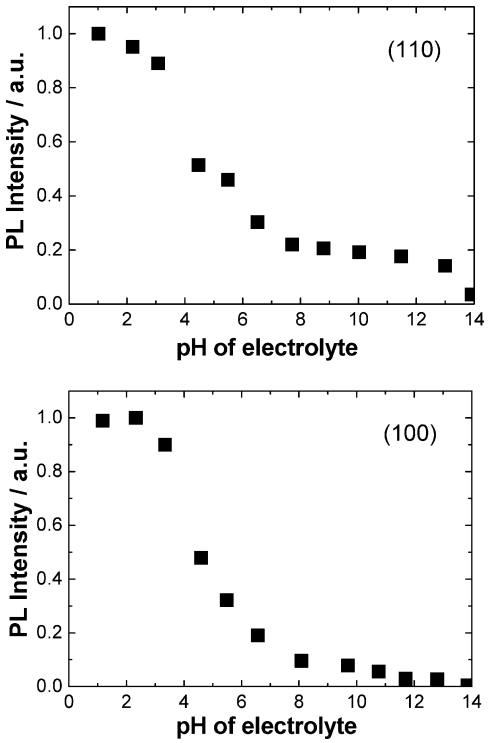

Figure 4. pH dependence of the I_{PL} for the n-TiO_2 (110) and (100) surfaces. The UV irradiation intensity was 0.2 mW/cm^2.

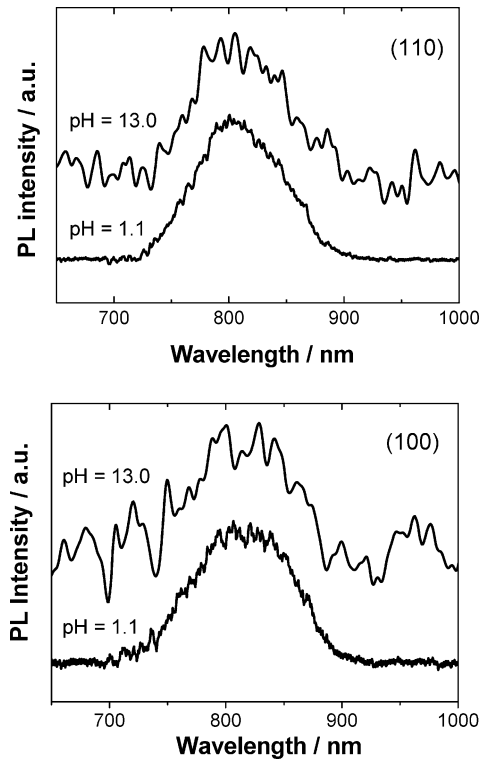

Figure 5. PL spectra from the (110) and (100) surfaces in 0.1 M $HClO_4$ (pH = 1.1) and 0.1 M NaOH (pH = 13.0). The peak intensities are normalized to the same level between pH 1.1 and 13.0.

PL-emitting species (surface-trapped hole, STH) is slightly different between the (100) and (110) surfaces.[53,54] An important result is that the PL spectra in pH 1.1 and 13.0 are identical with each other for both the (110) and (100) surfaces, indicating that the PL bands are arising from the same luminescent species (or the same electronic transition) all over the pH range, irrespective of expected changes in the forms of various surface O species by protonation and deprotonation.

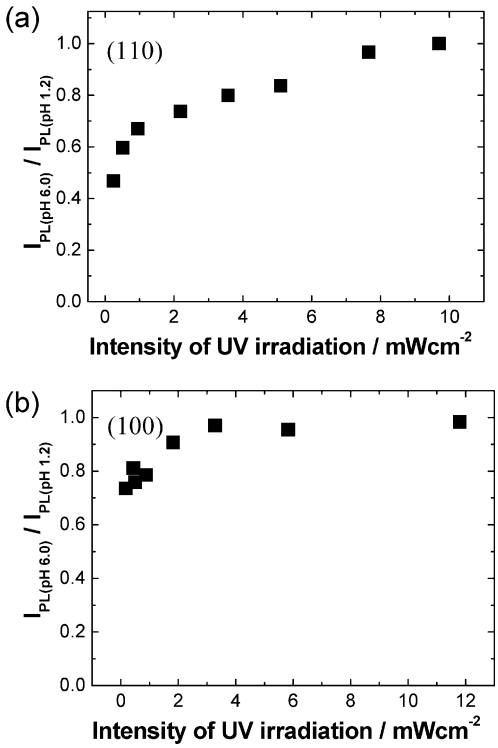

Figure 6. Ratio of the I_{PL} in pH = 6.0 to that in pH 1.2, plotted against the intensity of the UV irradiation.

The pH dependence of the I_{PL} was prominent under the low-intensity UV irradiation, as shown in Figure 4, but became less prominent at high illumination intensities. Figure 6 shows the irradiation-intensity dependence of the pH dependence of the I_{PL}, in which the ratio of the I_{PL} at pH 6.0 to that at pH 1.2 is plotted against the intensity of the UV irradiation. For both the (110) and (100) surfaces, the ratio increased with increasing the irradiation intensity and approached unity under the high irradiation intensities. In other words, under the high irradiation intensity, the I_{PL} became not to depend on the pH. The experimental data for the (100) surface under the low-intensity irradiation showed somewhat poor reproducibility, the ratio ranging in a region from 0.5 to 0.8, and thus the averaged value is plotted in Figure 6b.

Results similar to those of Figures 4−6 were obtained for other TiO_2 surfaces. Figure 7 shows the pH dependence of the I_{PL} and its irradiation-intensity dependence for an n-TiO_2 rutile electrode which was beforehand photoetched in 0.05 M H_2SO_4 and thus had the (100) surface.[51] The PL band emitted from suspensions of TiO_2 (rutile) particles, which were photoetched in 0.05 M H_2SO_4,[80] also showed a similar pH dependence.

As mentioned earlier, the atomic level surface roughening occurs with the progress of the water photooxidation reaction under anodic bias. We investigated how the solution pH affected the surface roughening. Figure 8 compares the AFM images of the atomically flat TiO_2(110) surfaces (a) before and (b, c) after the UV irradiation, during which the TiO_2 surface was immersed in (b) 0.1 M $HClO_4$ (pH 1.1) and (c) 0.1 M NaOH (pH 13.0). The irradiation was carried out at an intensity of 0.57 mW/cm^2

(80) Tsujiko, A.; Saji, Y.; Murakoshi, K.; Nakato, Y. *Electrochemistry* **2002**, *70*, 457−459.

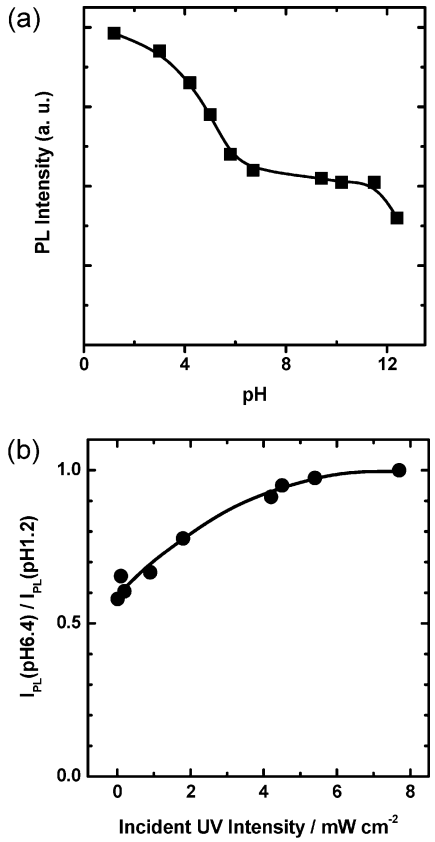

Figure 7. pH dependence of the I_{PL} and its illumination-intensity dependence for the n-TiO_2 rutile electrode, which was beforehand photoetched in 0.05 M H_2SO_4 and thus had the (100) face. The UV irradiation intensity was 0.2 mW/cm^2.

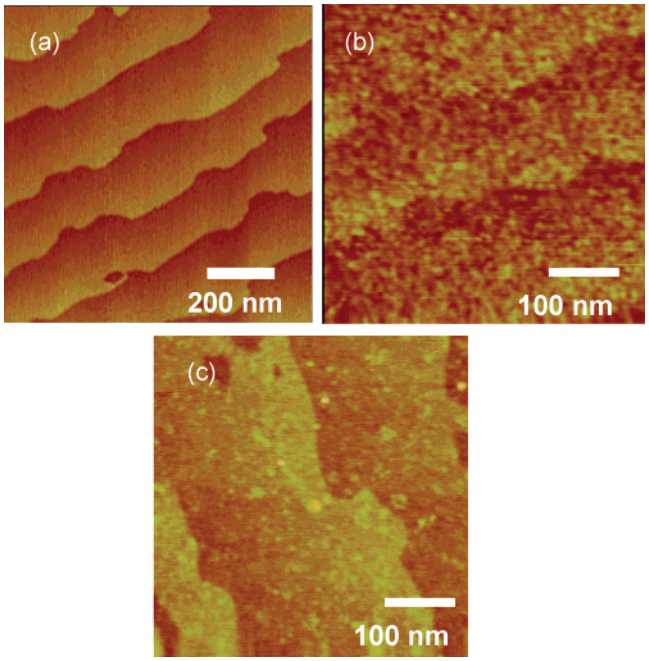

Figure 8. AFM images of the atomically flat n-TiO_2(110) surface (a) before and (b, c) after the UV irradiation, during which the TiO_2 surface was immersed in (b) 0.1 M $HClO_4$ (pH 1.1) and (c) 0.1 M NaOH (pH 13.0).

at the potential of 1.5 V vs Ag/AgCl/sat. KCl, and the electricity passing across the electrode surface was regulated to be 0.5 C/cm^2 in both the solutions. After the irradiation in 0.1 M $HClO_4$, a large number of tiny dots were formed at the TiO_2 surface, indicating that the serious surface roughening proceeded, as reported.[54] On the other hand, for the irradiation in 0.1 M NaOH, the atomic level flatness was retained fairly well, showing that the surface roughening was suppressed significantly in 0.1 M NaOH (a strongly alkaline aqueous solution). Some spots observed in Figure 8c are due to contaminations.

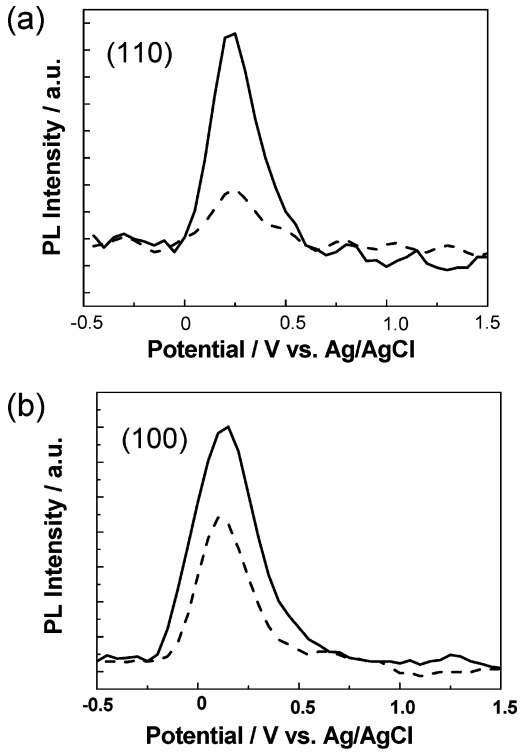

Figure 9. I_{PL} vs U for the (110) and (100) surfaces before (solid line) and after (broken line) addition of 0.1 M hydroquinone to the electrolyte (0.1 M $HClO_4$).

Figure 9 shows the effect of adding a reducing agent (hydroquinone) to the electrolyte (0.1 M $HClO_4$) on the I_{PL}. The I_{PL} for both the (110) and (100) surfaces was decreased by the addition of 0.1 M hydroquinone. The PL quenching can be explained by efficient electron transfer from hydroquinone to the surface-trapped holes (the luminescent species).[56,57] Especially, the I_{PL} for the (110) surface was more strongly decreased than that for the (100) surface, suggesting that the surface-trapped hole at the (110) surface is more easily reduced by hydroquinone than that at the (100) surface.

Discussion

To explain the pH dependence of the I_{PL}, let us first consider what oxygen species are present at the TiO_2 surface and how their densities change with the pH, on the basis of crystal lattice models for the TiO_2 (rutile) (110) and (100) surfaces (Figure 10) and reported studies.[66,75,81−83] For an electrically neutral surface under vacuum, one can assume triply coordinated oxygen atoms, [Ti−O=Ti_2] (species a in Figure 10), oxygen vacancies or five-coordinated Ti atoms, O_v (species b), and bridging oxygen atoms, [Ti−O−Ti] (species c), as main surface species. In the interior of TiO_2 crystal, a Ti^{4+} ion is coordinated with six O^{2-} ions and an O^{2-} ion is coordinated with three Ti^{4+}

(81) Henderson, M. A. *Langmuir* **1996**, *12*, 5093−5098.
(82) Schaub, R.; Thostrup, P.; Lopez, N.; Lægsgaard, E.; Stensgaard, I.; Nørskov, J. K.; Besenbacher, F. *Phys. Rev. Lett.* **2001**, *87*, 266104(1)−(4).
(83) Diebold, U. *Surf. Sci. Rep.* **2003**, *48*, 53−229.

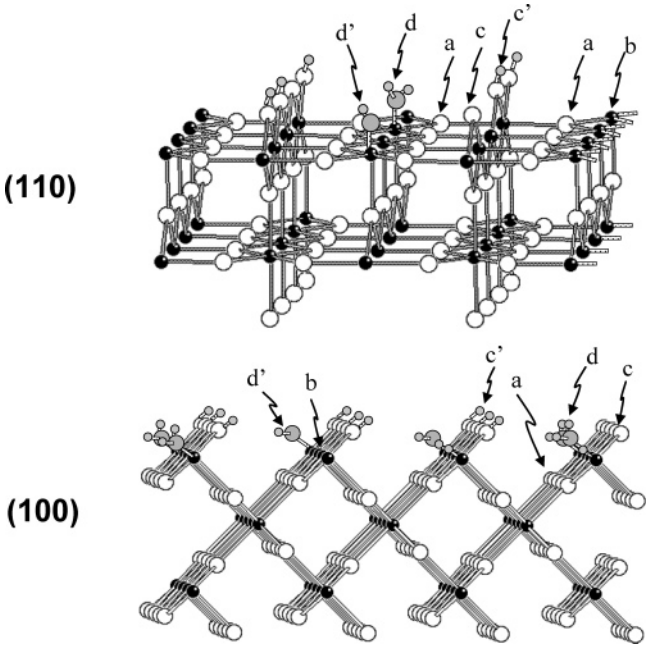

Figure 10. Crystal lattice models for the (110) and (100) surfaces: white circle, O^{2-}; black circle, Ti^{4+}; large gray circle, O atom of adsorbed water or OH; small gray circle, H atom.

ions. Accordingly, the surface oxygen vacancies or five-coordinated Ti atoms (species b) should have a formal charge of +(2/3)e (e: elementary charge), whereas the bridging oxygen atoms (species c) should have a formal charge of −(2/3)e. When the TiO_2 surface is in contact with an aqueous solution, water molecules are adsorbed at species b, producing $[Ti-OH_2]^{(2/3)+}$ (species d). Water molecules can also be dissociatively adsorbed at species b and c, producing $[Ti-OH]^{(1/3)-}$ (species d′) and $[Ti-OH-Ti]^{(1/3)+}$ (species c′).[66,81-83]

Of these surface species, it is sure that species a, $Ti_2=O-Ti$, at which the surface-trapped holes (STH) are formed (process 2), is present at the constant concentration throughout the pH range. It is also expected that the densities of protonated species such as $Ti-OH-Ti^{(1/3)+}$ and $Ti-OH_2^{(2/3)+}$ increase with decreasing the pH from the pzc (about 5.0[75,78,79]), whereas those of deprotonated species such as $Ti-O-Ti^{(2/3)-}$ and $Ti-OH^{(1/3)-}$ increase with increasing the pH. This argument is strongly supported by detailed studies on surface oxygen species on TiO_2 in a pH range 2.3−11.7 by internal reflection FTIR spectroscopy,[75] which reports that Ti−OH is present in a pH range from 4.3 to 10.7 (maximum ≅8), $Ti-OH_2^+$ exists in a pH range below 5, and $Ti-OH^+-Ti$ exists in a pH range below 4.3.

Well, how does the water oxidation reaction proceed at the TiO_2 surface? The prominent pH dependence of the I_{PL} (Figure 4) can be explained on the basis of the new mechanism, expressed by reactions 2−6 or Scheme 1. Let us first note that the assignment of the STH as the PL-emitting species is supported by the following many facts: (1) Species a, $Ti_2=O-Ti$, at which the STH is formed, is present throughout the pH range. (2) A sufficiently high probability of radiative recombination of electrons and holes is expected at a site of the STH, $[Ti-O=Ti_2]_s^+$, because it is still within the TiO_2 lattice and an overlap between Ti 3d and O 2p orbitals is significant. (3) No protonation or deprotonation occurs at $[Ti-O=Ti_2]_s^+$, namely, its chemical (and the electronic) structure is kept unchanged throughout the pH range, in agreement with no change in the spectral position and shape of the PL bands by the pH variation (Figure 5). (4) A slight difference in the spectral shape and position of the PL band between the (110) and (100) surfaces (Figure 5), i.e. a slight difference in the energy of the STH between these surfaces, is in agreement with a slight difference in the location and arrangement of the $[Ti-O=Ti_2]_s^+$ plane between these surfaces. Namely, the $[Ti-O=Ti_2]_s^+$ plane for the (110) surface is placed in parallel to the surface and directly exposed to the electrolyte, as is seen from Figure 10, whereas that for the (100) surface is placed slantwise to the surface and located a little inward from the surface, covered with adjacent adsorbed H_2O molecules and bridging O atoms (Figure 10). Such a difference in the location and arrangement should lead to a difference in the orientational polarization of water molecules in solution as well as crystal lattice relaxation against bond lengthening by trapping a hole. (5) The PL band from the (110) surface is much more effectively quenched by hydroquinone added to the electrolyte than that from the (100) surface (Figure 9). This result can also be attributed to the above-mentioned slight difference in the location and arrangement of the $[Ti-O=Ti_2]_s^+$ plane, because the difference should affect the rate of electron transfer from hydroquinone to the STH, which causes the PL quenching.

When the STH, $[Ti-O=Ti_2]_s^+$, is formed at the terrace, the direct nucleophilic attack of a H_2O molecule to the STH may be difficult because this reaction (insertion of OH into the Ti=O−Ti bond) should cause serious distortion of surface crystal lattice and have a large activation energy. Accordingly, it is assumed in Scheme 1 that the nucleophilic attack of H_2O occurs at surface bridging oxygen, $[Ti-O-Ti]_s$ (reaction 4), at which the distortion energy is expected to become much smaller. As mentioned in the Introduction, in reaction 4, an H_2O molecule attacks $[Ti-O-Ti]_s$, accompanied by transfer of a hole from $[Ti_2=O\cdots Ti]^+_s$ in a concerted manner. On the basis of this model, the pH dependence of the I_{PL} (Figures 3 and 4) can be explained quite reasonably as follows.

In an acidic solution (pH 1.1), the TiO_2 surface is mainly covered with $Ti-OH_2^{(2/3)+}$ and $Ti-OH-Ti^{(1/3)+}$, as mentioned earlier. The nucleophilic attack of a H_2O molecule to protonated bridging oxygen, $Ti-OH-Ti^{(1/3)+}$, will hardly occur because the positively charged STH cannot come close to such a positively charged species ($Ti-OH-Ti^{(1/3)+}$). Thus, the STH remains at the terrace for a while without causing any reaction, resulting in effective emission of the PL. The reaction of the STH may occur at nonprotonated bridging oxygen ($Ti-O-Ti^{(2/3)-}$) present at a very low density in terraces or kinks or steps. It is also highly probable that the accumulation of the STH with positive charges at the surface causes the downward shift of the surface band energies (or U_{fb}) of the n-TiO_2 electrode under anodic bias,[84] which accelerates deprotonation at $Ti-OH-Ti^{(1/3)+}$ and hence does the nucleophilic attack of H_2O. Note that the downward shift of the surface band energies (or U_{fb}) does not affect the rate of reaction 1 because the O 2p level for Ti−OH lying at the inner Helmholtz layer also shifts downward in parallel to the surface band energies (or U_{fb}).

With increasing the pH, the surface density of species c, $Ti-O-Ti^{(2/3)-}$, will increase by deprotonation. Thus, the rate of

(84) Nakanishi, S.; Tanaka, T.; Tsuji, E.; Fukushima, S.; Fukami, K.; Nagai, T.; Nakamura, R.; Imanishi, A.; Nakato, Y. *J. Phys. Chem. C* **2007**, *111*, 3934−3937.

reaction 4 via species c increases, resulting in the decrease in the density of the STH and hence in the lowering of the PL intensity (I_{PL}). This explanation is supported by the fact that the sharp decrease in the I_{PL} occurs at around pH 4, near the pzc of TiO_2 of about 5.0[75,78,79] (Figure 4). In fact, the internal reflection FTIR spectroscopic studies showed[75] that $Ti-OH^+-Ti$ existed in a pH range below 4.3, implying that the density of deprotonated $Ti-O-Ti^{(2/3)-}$ rapidly increases around pH = 4.

The pH dependence of the I_{PL} shows the second sharp decrease near pH 13 (Figure 4). This might tentatively be attributed to formation of readily oxidized species, $Ti-O^{(4/3)-}$, by deprotonation of species d′, f, and $Ti-OH^{(1/3)-}$, which can cause an electron-transfer reaction (see Scheme 1):

$$Ti-O^{(4/3)-} + h^+ \rightarrow Ti\text{-}O^{\bullet(1/3)-} \quad (7)$$

The formation of $Ti-O^{(4/3)-}$ in very high pH was suggested previously[85] from an increased cathodic current due to increased adsorbed oxygen molecules in a form of $Ti-O^-\cdots O_2$. The occurrence of reaction 7 in strongly alkaline solutions is also supported by AFM inspection of the TiO_2 surface, which showed that atomic level surface roughening was largely suppressed in pH 13 (Figure 8). As reaction 7 does not accompany any bond breaking at the surface crystal lattice, it is quite reasonable that the water oxidation reaction initiated by reaction 7 does not lead to the surface roughening.

It is worth noting here that the sharp decrease in the I_{PL} around pH 4 (Figure 4) is also in harmony with the assumption of reaction 1′ because the surface density of Ti−OH increases with the pH at around pH 4.[75] However, as already mentioned in the Introduction, reaction 1′ cannot explain previously reported experimental results of the incorporation of lattice oxygen into reaction intermediates[52] as well as photoinduced atomic level surface roughening.[54] As to the latter result, Figure 8 in this work shows interesting facts that the surface roughening which occurs in low pH is largely suppressed in high pH. The suppression can be attributed to the occurrence of reaction 7 in high pH, as argued above. This implies that the surface roughening in low pH cannot be explained by reaction 1′, which is a reaction of the same type as reaction 7. Moreover, the assumption of reaction 1′ cannot explain why the PL is emitted only from atomically flat TiO_2 (110) and (100) surfaces and not emitted from atomically *nonflat* surfaces (Figure 2). This experimental result indicates that atomically nonflat surfaces are much more reactive than atomically flat ones, but the assumption of reaction 1′ leads to the inverse conclusion because surface Ti−OH becomes less reactive (or less easily oxidized) with increasing atomic level surface roughening owing to decreased O 2p overlapping with lattice oxygen and decreased electronic polarization. The above argument is supported by blue shifts of the light absorption edge in a series of crystal TiO_2, amorphous TiO_2, and molecular $Ti(OH)_4$, i.e., in the order of increasing atomic level roughening. On the other hand, it is quite reasonable to expect that the nucleophilic attack of a water molecule for a surface hole is accelerated by atomic level surface roughening owing to a decrease in the activation energy induced by lattice distortion in a reaction site. Accordingly, we in this work conclude that reaction 4 or 5 is the main initiating step of the water oxidation reaction in low and intermediate pH, though the assumption of reaction 1′ might not be completely excluded at present.

The pH dependence of the I_{PL} becomes less prominent, i.e., the I_{PL} at pH 6.0 increases and approaches that at pH 1.2, under the high-intensity UV irradiation (Figure 6). This result can be explained as follows. Note first that the water photooxidation reaction proceeds stepwise via a number of surface reaction intermediates, as shown in Scheme 1. Note also that the surface bridging oxygen, Ti−O−Ti, at which the reaction is initiated, is reproduced only when the oxygen evolution is completed at the final step (Scheme 1). Now, under the high-intensity illumination, the hole flux to the surface is high and, thus, the initiating reaction, reaction 4, occurs efficiently one after another at pH 6.0. Accordingly, under a photostationary state at pH 6.0, most of the Ti−O−Ti species are changed to reaction intermediates or, in other words, the density of Ti−O−Ti becomes very low, which leads to the accumulation of the STH and the increase in the I_{PL}.

Finally, it is interesting to consider interrelations between reaction intermediates argued in this work and those reported by time-resolved laser spectroscopy,[86−88] though we should always keep in mind that samples used in these studies are not the same; i.e., this work uses single-crystal rutile TiO_2 with well-defined surfaces, whereas the spectroscopic work does nanocrystalline anatase TiO_2 particles with non-regulated surfaces. Very recently, Yoshihara et al. reported[87] that photogenerated holes produce two intermediate species, named hole-1 and hole-2 in ref 87: hole-1 shows the absorption band peaked at around 550 nm and is observed all over the pH range, whereas hole-2 shows the absorption band below 400 nm (probably peaked at around 350 nm) and is observed only in neutral and alkaline solutions. It is also reported[87,88] that hole-1 appears within the duration of a laser pulse, whereas hole-2 appears later with a delay, accompanied by the decay of hole-1.

These observations can be explained reasonably on the basis of the mechanism in this work, as explained below, if it is tentatively assumed that hole-1 corresponds to the STH and hole-2 corresponds to [Ti−OH ·O−Ti] radicals. First, the delayed appearance of hole-2, accompanied by the decay of hole-1, is in good agreement with processes of reactions 2−4. Second, the assignment of hole-2 to [Ti−OH ·O−Ti] radical is supported by the reported fact[89] that the reaction of ·OH radicals with TiO_2 particles gives a spectrum similar to that of hole-2, because it is very likely that the reaction of ·OH radicals with surface Ti−O−Ti leads to the formation of [Ti−OH ·O−Ti]. Third, it is also plausible that the STH shows an absorption band in the visible region because the STH, $[Ti-O{=}Ti_2]_s^+$, has a vacant O 2p orbital, to which an electron lying deep in the valence band can be excited. This absorption band can also be interpreted as a red-shift of the ∼250-nm band ($A^2\Sigma^+ \leftarrow X^2\Pi$ transition) for the $HO^\bullet$ radical[47,90] (or the ∼350-nm band for surface $Ti-O^\bullet$ radical[89]) caused by the incorporation of the

(85) Tsujiko, A.; Itoh, H.; Kisumi, T.; Shiga, A.; Murakoshi, K.; Nakato, Y. *J. Phys. Chem. B* **2002**, *106*, 5878−5885.
(86) Shkrob, I. A.; Sauer, M. C., Jr. *J. Phys. Chem. B* **2004**, *108*, 12497−12511.
(87) Yoshihara, T.; Tamaki, Y.; Furube, A.; Murai, M.; Hara, K.; Katoh, R., *Chem. Phys. Lett*. **2007**, *438*, 268−273.
(88) Yang, X.; Tamai, N. *Phys. Chem. Chem. Phys*. **2001**, *3*, 3393.
(89) Lawless, D.; Serpone, N.; Meisel, D. *J. Phys. Chem.* **1991**, *95*, 5166.
(90) Thomas, J. K.; Rabani, J.; Matheson, M. S.; Hart, E. J.; Gordon, S. *J. Phys. Chem*. **1966**, *70*, 2409.

radical into surface TiO_2 lattice (or by the mixing of O 2p orbitals of the radical with those of the valence band). Fourth, the absorption band assigned to hole-1 is observed all over the pH range, whereas the absorption band assigned to hole-2 is observed only in neutral and alkaline solutions and missing in low pH. The appearance of the hole-1 band all over the pH range is in harmony with the fact that the STH or triply coordinated surface lattice oxygen, $[Ti-O=Ti_2]_s$, exists throughout the pH range. The missing of the hole-2 band in low pH can be explained by taking into account that almost all surface bridging oxygen is protonated in low pH, thus leading to no production of [Ti−OH ·O−Ti] radical in TiO_2 particles. For an n-TiO_2 electrode (with upward band bending) under an anodic bias, on the other hand, the accumulation of the STH (with a positive charge) can occur at the surface, which causes the downward shift of the surface band energies (or U_{fb}), which in turn accelerates deprotonation at $Ti-OH-Ti^{(1/3)+}$ and hence the nucleophilic attack of H_2O, as argued earlier. We can, however, expect no accumulation of the STH in particulate TiO_2 systems, in which no band bending is present and efficient carrier recombination occurs. Now, we can see that this work and time-resolved spectroscopic studies give results in harmony with each other. Further studies are, however, needed to get definite conclusions.

Conclusion

This work has confirmed that the PL bands, peaked at around 810 and 840 nm at the atomically flat (110) and (100) surfaces, respectively, can be assigned to radiative recombination transitions between the conduction-band electrons and surface-trapped holes (STH), $[Ti-O=Ti_2]_s^+$, formed at triply coordinated O atoms at the surface lattice. The PL intensity (I_{PL}) decreased stepwise with increasing the solution pH; namely, it sharply decreased at around pH 4, near the point of zero charge of TiO_2 (about 5.0), and then rapidly decreased to zero near pH 13. The first sharp decrease near pH 4 was explained reasonably by taking into account the pH dependence of the densities of surface O species, on the basis of our previously proposed new mechanism that the water photooxidation reaction was initiated by nucleophilic attack of water molecules to the STH at surface bridging O atoms. The second sharp decrease near pH 13 was attributed to formation of surface $Ti-O^-$ which was readily oxidized by photogenerated holes. These results on the pH dependence of the I_{PL} thus give strong support to our previously proposed new mechanism for the water photooxidation reaction. The new mechanism has quite different energetic and kinetics from the conventional electron-transfer-type mechanism and will serve for exploring new efficient visible-light responsive photoelectrodes and photocatalysts for the decomposition of water and organic compounds.

JA073206+